*Geophysical Research Letters*

Supporting Information for

# Evaluation of ocean surface waves along the coastal area of the Sea of Okhotsk during winter

S. Iwasaki[1] and J. Otsuka[1]

[1] Civil Engineering Research Institute for Cold Region, 1-3-1-34 Toyohira, Sapporo 062-8602, Japan

## Contents of this file



## Introduction

This supporting information provides additional text, figures, and tables for more detailed methods and results.

### Text S1. Wave–ice models in WW3

A brief overview of six wave–ice parameterization models, denoted as IC0–IC5 in WW3, and the ice parameters used in this study, are provided here. Fundamentally, we used the default values of ice parameters following the WW3 manual.

IC0 is based on Tolman (2003) and provides a simple blocking of energy flux depending on the local ice concentration. IC1 allows the user to provide an exponential attenuation rate of amplitude, uniform in the frequency space (Rogers and Orzech, 2013). IC2 assumes dissipation by friction in the boundary layer below the ice cover (Liu and Mollo-Christensen, 1988). IC3 treats the ice cover as a linear viscoelastic layer, based on the model by Wang and Shen (2010). IC4 was introduced by Collins and Rogers (2017) and provides the dissipation of wave energy by one of the several simple, empirical, and parametric forms through direct fitting with field data. In addition, IC5 uses a viscoelastic model based on Mosig et al. (2015). $k_{\mathrm{i}}$ is implemented for source functions in IC1–5, except for IC0. The estimation of $k_{\mathrm{r}}$ requires IC2, IC3, and IC5 to provide a new dispersion relation. A description of these models is provided below.

IC0 was updated by Tolman (2003) to a "continuous treatment" to allow partial blocking of partial ice cover. In this method, a user defines two critical ice concentrations that describe the minimum concentration that affects the waves ($C_{\mathrm{i},0}$), and the concentration at which the wave

energy is completely blocked ($C_{\mathrm{i,n}}$). For the ice concentration between $C_{\mathrm{i,0}}$ and $C_{\mathrm{i,n}}$, the wave energy is partially blocked or transmitted based on linear interpolation between the two values. In the present study, these critical ice concentrations are $C_{\mathrm{i,0}}$= 0.25, and $C_{\mathrm{i,n}}$= 0.75. IC0 does not treat the effect as "dissipation" via the $S_{\mathrm{ice}}$ source function, but rather as a feature of the propagation schemes. In addition, this method does not permit variation in the dissipation rate with frequency. The details of IC0 can be found in Tolman (2003).

IC1 is the first $S_{\mathrm{ice}}$ source function in WW3, based on Rogers and Orzech (2013). In this source term, the user provides the exponential attenuation rate ($k_{\mathrm{i}}$) of the wave amplitude with distance. The attenuation rate did not vary with the frequency space. In the present study, $k_{\mathrm{i}}$ = $2 \times 10^{-5}$ is used.

IC2 is based on the method proposed by Liu and Mello-Christensen (1988). This model is derived based on the assumption that dissipation is caused by turbulence in the boundary layer between the ice and the water layer, with the ice modeled as a continuous thin elastic plate. The input parameters are the ice thickness ($h_{\mathrm{i}}$) and kinematic viscosity ($\nu$) in the boundary layer beneath the ice. The dispersion relation of IC2 is defined as:

$$\sigma^2 = \frac{\mathrm{g}k_{\mathrm{r}} + Bk_{\mathrm{r}}^5}{\coth(k_{\mathrm{r}}d) + (k_{\mathrm{r}}M)}, \tag{1}$$

$$C_{\mathrm{g}} = \frac{\mathrm{g} + (5 + 4k_{\mathrm{r}}M)Bk_{\mathrm{r}}^5}{2\sigma(1 + k_{\mathrm{r}}M)^2}, \tag{2}$$

$$\alpha = \frac{\sqrt{\nu\sigma}k_{\mathrm{r}}}{C_{\mathrm{g}}\sqrt{2}(1 + k_{\mathrm{r}}M)}, \tag{3}$$

where g is the gravitational acceleration, and $d$ is the water depth. $B$ and $M$ denote the effects that modify the frequency owing to the bending of the ice and the inertia of the ice, respectively. $B$ and $M$ depend on the ice thickness ( Liu and Mello-Christensen, 1988; Liu et al., 1991 for details). In the present study, we used a ν value of $1536 \times 10^{-4}$ m$^2$ s$^{-1}$) for $\nu$.

IC3 employs the viscoelastic model proposed by Wang and Shen (2010). IC3 theorizes that ice can store and dissipate energy; thus, the model assumes ice as a viscoelastic layer. The storage property is reflected in the potential and elastic energy, and the dissipative property is equivalent to viscous damping. The dispersion relation of IC3 can be described as:

$$\sigma^2 - Q\mathrm{g}k\tanh(kd) = 0, \tag{4}$$

$$Q = 1 + \frac{\rho_{\mathrm{i}}}{\rho_{\mathrm{w}}}\frac{(\mathrm{g}^2k^2 - K^4 + 16k^6a^2\nu_e^4)S_kS_a - 8k^3a\nu_e^2(C_kC_a - 1)}{\mathrm{g}k(4k^3a\nu_e^2S_kC_a + K^2S_aC_k - \mathrm{g}kS_kS_a)}. \tag{5}$$

In the above, $a^2 = k^2 - i\sigma/\nu_e$, $S_k = sinh(kh_{\mathrm{i}})$, $S_a = sinh(ah_{\mathrm{i}})$, $C_k = cosh(kh_{\mathrm{i}})$, $C_a = cosh(ah_{\mathrm{i}})$, $K = \sigma + 2ik^2\nu_e$, $\nu_e = \nu + iG/\rho_{\mathrm{i}}\sigma$. $\rho_{\mathrm{w}}(\rho_{\mathrm{i}})$ is the density of water (sea ice). $\rho_{\mathrm{w}}$ is 1025 kg m$^{-3}$ in this study. The IC3 model requires four ice parameters: ice thickness, kinematic viscosity, ice density, and effective shear modulus ($G$). In this study, we have implemented values of, $\nu$ = 1.0 (m$^2$ s$^{-1}$), $\rho_{\mathrm{i}} = 917$ (kg m$^{-3}$), $G$ =$1.0 \times 10^3$ (Pa).

The concept of IC4 is a simple, efficient, and flexible implementation of frequency-or period-dependent wave attenuation. Details of IC4 were introduced by Collins and Rogers (2017). There are seven methods in IC4, denoted as IC4M1–M7, as follows:

IC4M1 has an exponential equation that fits the data of Wadhams et al. (1988). The equation is as follows:

$$\alpha = exp[-C_1 T - C_2], \tag{6}$$

where $T = 2\pi/\sigma$ is the wave period. Following Wadhams et al. (1988), we used the following parameters: $C_1 = 0.18$, $C_2 = 7.3$.

IC4M2 is polynomial fit depend on frequency ($f$ =1/ $T$) as follows:

$$\alpha = C_1 + C_2 f + C_3 f^2 + C_4 f^3 + C_5 f^4. \tag{7}$$

In this method, the dissipation is represented using a user-specified polynomial. Thus, it is a flexible method as a user has the freedom to change all the coefficients of the polynomial; in this case, it is the shape of the attenuation function. In this study, we used the coefficients ($C_3$ and $C_5$) of binomial fitting suggested by Meylan et al. (2014), Rogers et al. (2018), and Rogers et al. (2021) (Table S1). Thus, eight simulation cases were conducted for IC4M2. IC4M6H1–H3 used the coefficients of the binomial equation fitted to the step functions of IC4M6, as shown in Table S2. Surface Wave Instrument Float with Tracking (SWIFT) buoy (Thomson 2012), U.K. wave buoy (Wadhams and Thomson 2015), and National Institute of Water and Atmospheric Research (NIWA) buoy (Kohout et al. 2015) from Wave Array 3 (WA3) of the Office of Naval Research (ONR) "Sea State" experiment are used for the parameterizations of IC4M2. See Rogers et al. (2018) for details on IC4M6H1, IC4M6H2, IC4M6H3, WA3 SWIFT, WA3 UK, and WA3 NIWA in Table S1.

IC4M3 is based on the work of Horvat and Tziperman (2015). Horvat and Tziperman (2015) fitted a quadratic equation to the attenuation coefficient calculated by Kohout and Meylan (2008), depending on the wave period ($T = 1/f$) and ice thickness ($h_\mathrm{i}$). The attenuation rate increases as the wave period and ice thickness increase. This equation has the following form:

$$\ln \alpha = -0.3203 + 2.058 h_\mathrm{i} - 0.9375 T - 0.4269 h_\mathrm{i}^2 + 0.1566 h_\mathrm{i} T + 0.0006 T^2. \tag{8}$$

Attenuation of IC4M4 is a function of the significant wave height ($H_\mathrm{s}$) (Kohout et al. 2014):

$$\frac{dH_\mathrm{s}}{dx} = \begin{cases} C_1 \times H_s & \text{for } H_s \le 3\ m \\ C_2 & \text{for } H_s > 3\ m' \end{cases} \tag{9}$$

Here, $k_\mathrm{i} = dH_s/dx$. The attenuation rate increases linearly with $H_s$ until $H_s$= 3 m, regardless of the frequency. Following Kohout et al. (2014), $5.35 \times 10^{-6}$ and $16.05 \times 10^{-6}$ are used for $C_1$ and $C_2$, respectively.

IC4M5 provides attenuation as a step function in the frequency space in four steps. This method is provided by nonstationary and nonuniform parameters ($C_1 - C_7$). $C_1 - C_4$ determines the values of attenuation ($k_\mathrm{i}$) at each step, and $C_5 - C_7$ controls the end of the frequency range (given in Hz) of the first three steps. However, this method was not used in this study because IC4M5 cannot set the step function more finely than IC4M6, as shown below.

IC4M6 is also a step function similar to IC4M5, but has a frequency space of 10 steps.

Furthermore, it is a spatiotemporally constant step function. In this method, such as IC4M5, a user defines the attenuation rate ($k_\mathrm{i}$) at each step and the end of the frequency range (in Hz). In the present study, six simulation cases were performed, as shown in Table S2. The values in Table S2 are the parameters proposed by Rogers et al. (2018). "WA3 Doble" in Table S2 is based on the data of Doble et al. (2015).

IC4M7 uses the monomial expression for dissipation by Doble et al. (2015). Similarly, for IC4M3, the equation depends on wave period ($T$) and ice thickness ($h_\mathrm{i}$):

$$\alpha = 0.2T^{-2.13}h_\mathrm{i}. \tag{10}$$

IC5 is based on a viscoelastic beam model of Mosig et al. (2015). Relation of Eq. (4) is the same as IC3, while estimation of $Q$ is different as follow:

$$Q = \frac{G_\nu h_\mathrm{i}^3}{6\rho_\mathrm{w}\mathrm{g}}(1+V)k^4 - \frac{\rho_\mathrm{i}h_\mathrm{i}\sigma^2}{\rho_\mathrm{w}\mathrm{g}} + 1, \tag{11}$$

where $G_\nu = G - i\sigma\rho_\mathrm{i}\nu$ is the complex shear modulus, and $V$ is the Poisson's ratio (0.3) of ice. IC5 is also a viscoelastic model, similar to IC3. However, IC3 is an extension of the viscous ice layer model with a finite thickness (Keller, 1998), which includes elasticity into a complex viscosity (Wang and Shen, 2010). In contrast, IC5 is an extension of the thin elastic plate model (Fox and Squire, 1994) introduced by Mosig et al. (2015) by adding viscosity to a complex shear modulus. Similar to IC3, the input parameters of IC5 are ice thickness, kinematic viscosity, ice density, and effective shear modulus. The parameters used were as follows: $\nu = 5.0 \times 10^7$ ($\mathrm{m^2\ s^{-1}}$), $\rho_\mathrm{i} = 917$ ($\mathrm{kg\ m^{-3}}$), and $G = 4.9 \times 10^{12}$ (Pa).

**Text S2. Buoy observation**

To validate the model results of the wave field, we used buoy observation data from the Nationwide Ocean Wave Information Network for Ports and Harbours (NOWPHAS; http://www.mlit.go.jp/kowan/nowphas/index_eng.html), provided by the Ports and Harbours Bureau, Ministry of Land, Infrastructure, Transport, and Tourism (MLIT). Significant wave height and period data obtained every 20 min were used for the observation depth of 52.6m in the Monbetsu (south) Station (blue dot in Fig.1h). The buoy data were used for the three years during 2008–2010, similar to the model results. In the present study, the observation data were averaged from 20 min to 1 h, when compared with the simulation results.

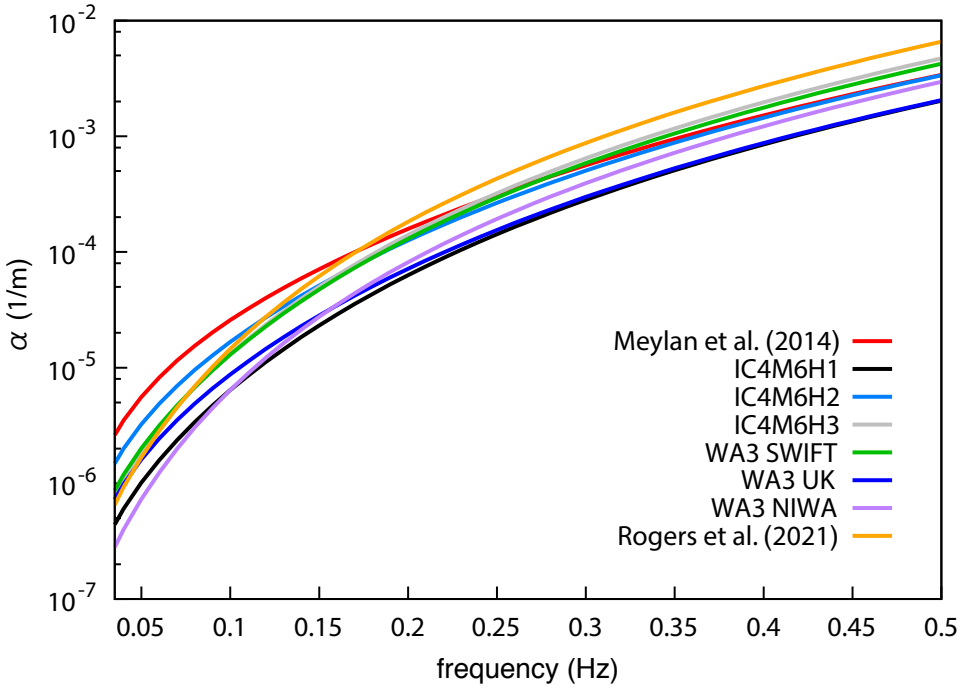


**Figure S1.** Attenuation rate ($\alpha$) as a function of frequency for eight binomial functions of IC4M2 employed in this study. The line colors are defined in the legend in the lower right corner.

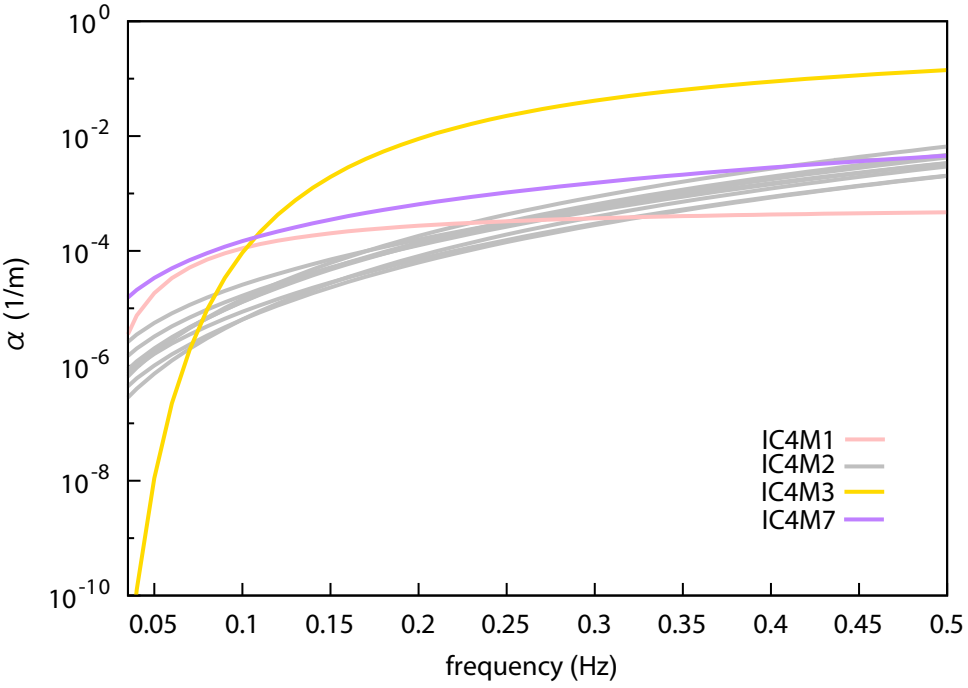


**Figure S2.** Attenuation rate ($\alpha$) as a function of frequency for four binomial functions of IC4M1, IC4M2, IC4M3, and IC4M7 employed in this study. The line colors are defined in the legend in the lower right corner. In this figure, $h_i = 5$ cm is used for IC4M3 and IC4M7. Gray lines show the eight binomial functions of IC4M2 in Figure S1.

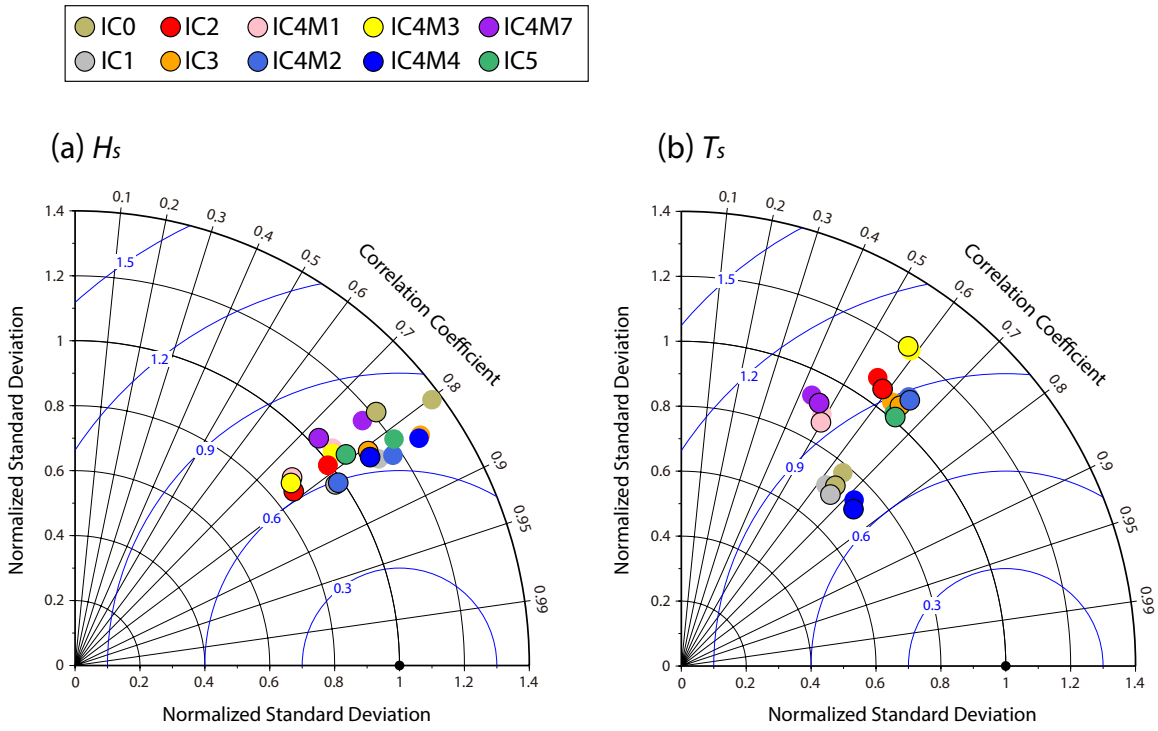


**Figure S3.** Same as Figure 2 but with model results with ST4 (markers with black outlines). ST6 simulations (markers without black outlines) in Figure 2 also shown in both figures.

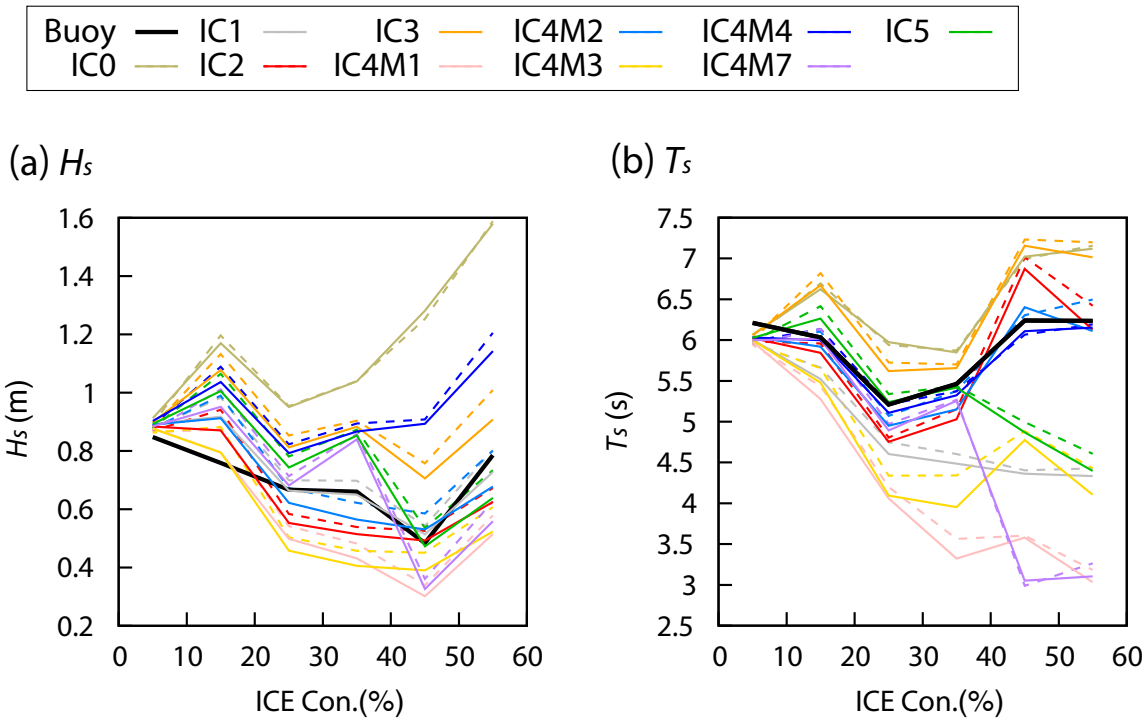


**Figure S4.** Same as Figure 3 but for model results with ST4 (colored lines). ST6 simulations (broken colored lines) in Figure 3 also indicated in both figures.

| Name | $C_3$ | $C_5$ |
|---|---|---|
| Meylan et al. (2014) | 2.120.E-03 | 4.590.E-02 |
| IC4M6H1 | 3.280.E-04 | 3.120.E-02 |
| IC4M6H2 | 1.176.E-03 | 4.920.E-02 |
| IC4M6H3 | 5.800.E-04 | 7.320.E-02 |
| WA3 SWIFT | 6.420.E-04 | 6.520.E-02 |
| WA3 UK | 5.680.E-04 | 3.060.E-02 |
| WA3 NIWA | 1.758.E-04 | 4.660.E-02 |
| Rogers et al. (2021) | 4.160.E-04 | 1.036.E-01 |

**Table S1.** Values of $C_3$ and $C_5$ for IC4M2 used in this study.

| Frequency range (Hz) | IC4M6H1 | IC4M6H2 | IC4M6H3 | WA3 SWIFT | WA3 Doble | WA3 NIWA |
|---|---|---|---|---|---|---|
| | $k_\mathrm{i}$ (1/m) | | | | | |
| 0.035-0.045 | 1.00.E-06 | 1.00.E-06 | 1.00.E-06 | 1.00.E-06 | 1.00.E-06 | 1.00.E-06 |
| 0.045-0.055 | 2.00.E-06 | 2.00.E-06 | 2.00.E-06 | 2.00.E-06 | 2.00.E-06 | 2.00.E-06 |
| 0.055-0.100 | 2.94.E-06 | 5.10.E-06 | 4.22.E-06 | 4.48.E-06 | 4.92.E-06 | 2.13.E-06 |
| 0.100-0.150 | 4.27.E-06 | 1.50.E-05 | 1.24.E-05 | 1.12.E-05 | 5.80.E-06 | 3.86.E-06 |
| 0.150-0.200 | 7.95.E-06 | 3.00.E-05 | 2.26.E-05 | 2.28.E-05 | 8.62.E-06 | 1.46.E-05 |
| 0.200-0.250 | 2.95.E-05 | 6.40.E-05 | 6.92.E-05 | 6.91.E-05 | 3.28.E-05 | 5.47.E-05 |
| 0.250-0.300 | 1.12.E-04 | 1.50.E-04 | 2.24.E-04 | 2.06.E-04 | 9.70.E-05 | 1.59.E-04 |
| 0.300-0.350 | 2.74.E-04 | 3.40.E-04 | 5.80.E-04 | 5.08.E-04 | 2.59.E-04 | 3.25.E-04 |
| 0.350-0.400 | 4.95.E-04 | 7.50.E-04 | 1.10.E-03 | 9.33.E-04 | 5.51.E-04 | 5.68.E-04 |
| 0.400-1.100 | 8.94.E-04 | 1.40.E-03 | 1.94.E-03 | 1.69.E-03 | 1.00.E-03 | 1.32.E-03 |

**Table S2.** $k_\mathrm{i}$ values for each frequency range of IC4M6 used in this study.

| | Meylan et al. (2014) | IC4M6H1 | IC4M6H2 | IC4M6H3 | WA3 SWIFT | WA3 UK | WA3 NIWA | Rogers et al. (2021) |
|---|---|---|---|---|---|---|---|---|
| $H_s$ | | | | | | | | |
| Bias (m) | 0.03 | 0.20 | 0.08 | 0.10 | 0.10 | 0.17 | 0.18 | 0.07 |
| RMSE (m) | 0.40 | 0.44 | 0.40 | 0.41 | 0.41 | 0.42 | 0.44 | 0.41 |
| Corr. | 0.82 | 0.84 | 0.83 | 0.83 | 0.84 | 0.84 | 0.83 | 0.83 |
| $T_s$ | | | | | | | | |
| Bias (s) | -0.34 | 0.62 | 0.02 | 0.17 | 0.19 | 0.46 | 0.61 | 0.09 |
| RMSE (s) | 1.94 | 2.00 | 1.96 | 2.01 | 2.00 | 1.97 | 2.04 | 2.03 |
| Corr. | 0.65 | 0.61 | 0.65 | 0.64 | 0.64 | 0.63 | 0.61 | 0.64 |

**Table S3.** Statistical values of $H_s$ and $T_s$ between IC4M2 simulations and buoy observation.

| | IC4M6H1 | IC4M6H2 | IC4M6H3 | WA3 SWIFT | WA3 Doble | WA3 NIWA |
|---|---|---|---|---|---|---|
| $H_s$ | | | | | | |
| Bias (m) | 0.24 | 0.10 | 0.12 | 0.12 | 0.20 | 0.23 |
| RMSE (m) | 0.44 | 0.40 | 0.41 | 0.41 | 0.42 | 0.45 |
| Corr. | 0.83 | 0.84 | 0.84 | 0.84 | 0.84 | 0.83 |
| $T_s$ | | | | | | |
| Bias (s) | 0.60 | 0.08 | 0.21 | 0.23 | 0.46 | 0.73 |
| RMSE (s) | 1.88 | 1.92 | 1.92 | 1.92 | 1.97 | 1.98 |
| Corr. | 0.62 | 0.65 | 0.64 | 0.64 | 0.63 | 0.60 |

**Table S4.** Comparison statistics of $H_s$ and $T_s$ by IC4M6 simulations with buoy observation.

| | IC0 | IC1 | IC2 | IC3 | IC4M1 | IC4M2 | IC4M3 | IC4M4 | IC4M7 | IC5 |
|---|---|---|---|---|---|---|---|---|---|---|
| $H_s$ | | | | | | | | | | |
| Bias (m) | 0.46 | 0.04 | -0.04 | 0.22 | -0.13 | 0.01 | -0.13 | 0.25 | 0.05 | 0.11 |
| RMSE (m) | 0.49 | 0.37 | 0.39 | 0.41 | 0.41 | 0.37 | 0.41 | 0.40 | 0.46 | 0.42 |
| Corr. | 0.77 | 0.82 | 0.78 | 0.81 | 0.76 | 0.82 | 0.76 | 0.82 | 0.73 | 0.79 |
| $T_s$ | | | | | | | | | | |
| Bias (s) | 0.64 | -0.95 | -0.20 | 0.54 | -1.64 | -0.16 | -1.16 | -0.08 | -0.87 | -0.32 |
| RMSE (s) | 1.70 | 1.68 | 2.08 | 1.93 | 2.10 | 1.94 | 2.29 | 1.50 | 2.22 | 1.87 |
| Corr. | 0.65 | 0.66 | 0.59 | 0.64 | 0.50 | 0.65 | 0.58 | 0.74 | 0.46 | 0.65 |

**Table S5.** Same as Table 1 but for the model simulations with ST4.